A Stabilized Finite Element Formulation for Continuum Models of Traffic Flow

Durgesh Vikram[1]**, Sanjay Mittal**[2] **and Partha Chakroborty**[1]

Abstract: A stabilized finite element formulation is presented to solve the governing equations for traffic flow. The flow is assumed to be one-dimensional. Both, PW-type (Payne-Whitham) 2-equation models and the LWR-type (Lighthill-Whitham-Richards) 1-equation models are considered. The SUPG (Streamline-Upwind/Petrov-Galerkin) and shock capturing stabilizations are utilized. These stabilizations are sufficient for the 1-equation models. However, an additional stabilization is necessary for the 2-equation models. For the first time, such a stabilization is proposed. It arises from the coupling between the two equations and is termed as IEPG (Inter-Equation/Petrov-Galerkin) stabilization. Two behavioral models are studied: Greenshields' (*GS*) and Greenberg's (*GB*) models. Numerical tests are carried out for cases involving traffic expansion as well as shock. Excellent agreement with the exact solution is observed. The need of the IEPG stabilization for the 2-equation traffic models is demonstrated. An interesting observation is made for the first time regarding the Greenberg's (GB) model in the presence of a shock. The model is found to be inconsistent in the sense that it leads to different shock speed from the continuity and behavior equations. As a result, the 2-equation model leads to secondary waves in the presence of shocks.

Keywords: Traffic flow, Finite element method, (IEPG) Inter-Equation/Petrov-Galerkin stabilization, SUPG, Shock wave, Expansion wave.

1   Introduction

Traffic facilities can be designed effectively only when engineers have a good insight into how traffic flows and have tools to analyze how this flow gets affected by different design parameters. Hence, it is important to model traffic flow. There

---

[1] Department of Civil Engineering, Indian Institute of Technology Kanpur, U.P. 208016, INDIA, Ph:+91 512 2597037.

[2] Department of Aerospace Engineering, Indian Institute of Technology Kanpur, U.P. 208016, INDIA, Ph:+91 512 2597906.

are two different modelling frameworks which are used to represent flow of traffic; namely, the microscopic modelling framework (or simply the microscopic models) and the macroscopic models.

In the group of models known as microscopic models, vehicle-vehicle interactions are modelled. The behaviour of the traffic stream is obtained through an agglomeration of these individual vehicle-vehicle interactions. [Brackstone and McDonald (2000)] gives a good overview of the important models in this class. Although these models are appealing, as they seek to explicitly incorporate the driver behaviour, they cannot be used to study streams of any realistic size. [Zang (1998)] also mentions a similar point.

Macroscopic models, on the other hand, try to describe the collective effects of the vehicle-vehicle interactions in terms of stream parameters like speed, flow, and density. The importance of this modelling framework, which can be used to study streams of realistic sizes, in helping engineers design efficient traffic facilities, cannot be overstated. Continuum models of traffic flow, which treat traffic streams as a continuum and uses analogies with fluid flow theories, belong to the class of macroscopic models. Two broad classes of continuum models exist. In one the traffic stream is modelled as one which satisfies the continuity equation and an assumed (user-specified) speed-density relation; these models are also referred to as the LWR models (see [Lighthill and Whitham (1955) and Richards (1956)]). In the other, in addition to the continuity equation the model includes a description of driver behaviour in terms of driver acceleration in response to the density state of the road in the near vicinity and some other factors; these 2-equation models are often referred to as PW models [Payne (1971) and Whitham (1974)]; Greenbergs model [Greenberg (1959)] also falls in this class.

Unfortunately, the current state of the paradigm of 2-equation continuum models of traffic flow is, as [Papageorgiou (1998)] puts it, (characterized by the existence of diverging views with regard to the theoretical soundness and the practical usefulness). Given the importance of such a modelling framework in traffic engineering the authors have made another attempt to look into the 2-equation model of traffic flow, both analytically and numerically, with an aim to identifying the cause of some of the shortcomings reported in the literature and suggest improvements.

Unlike several earlier studies [Zhang (2001), Leo and Pretty (1992), Zhang and Wong (2006), Michalopoulos, Beskos, and Lin (1984), Daganzo (1995), Jiang, Wu, and Zhu (2002) and Liu (2006)], this study uses the finite element method for solving the equations governing the traffic flow. Specifically, this study develops a stabilized finite element formulation for the LWR and 2-equation models. To handle instabilities arising out of convection term, the well known SUPG (Streamline-Upwind/Petrov-Galerkin) stabilization [Brooks and Hughes (1982)],

is used. For instabilities that arise due of the presence of shocks, or regions of very high spatial gradients, a stabilization is developed. The additional stabilization terms added to the formulation are referred to as the shock capturing terms. The development of these is inspired by the work reported in several earlier articles [Juanes and Patzek (2005), Beau and Tezduyar (1991), Mittal (1998a) and Mittal (1998b)]. In the 2-equation models, it is found that these two sets of stabilizations are not enough. The coupling between the variables in the two equations leads to another instability. A new set of terms are added to the formulation that stabilize the computations against these instabilities. We refer to this stabilization as the IEPG (Inter-Equation/Petrov-Galerkin) stabilization. The effectiveness of the stabilized formulation is demonstrated via a variety of test cases.

The paper is divided into five sections of which this is the first. The LWR and 2-equation models of traffic flow are presented in Section 2. Section 3 discusses in detail the numerical formulation for the models presented in Section 2. Results from the test cases are discussed in Section 4. The last section concludes the paper by summarizing the work done here and highlighting the contributions.

2 The governing equations

2.1 2-equation models

The unsteady flow of traffic along a road is considered. The traffic is assumed to be one-dimensional. Let x denote the space and t, the time. Let $k(x,t)$ be the density of traffic defined as number of vehicles per unit length of the road and $u(x,t)$, the traffic speed. The flux of the traffic is defined as $q = ku$. A typical traffic model is based on (a) the conservation of number of vehicular units, and (b) the driver behavior. The conservation law for the volume of vehicles can be expressed as:

$$\frac{\partial k}{\partial t} + \frac{\partial q}{\partial x} = 0 \tag{1}$$

Equation (1) assumes that there is no entry/exit ramp to the road being considered. The behavior of the driver impacts the acceleration/deceleration of the vehicle and can be expressed as:

$$\frac{\partial u}{\partial t} + u\frac{\partial u}{\partial x} = A(k,u) \tag{2}$$

The term on the right hand side of Equation (2) is usually of the form $A(k,u) = -a(k,u)\frac{\partial k}{\partial x}$. The acceleration of the vehicle is related to the spatial gradient of the traffic density, $\frac{\partial k}{\partial x}$. The driver accelerates the vehicle if the traffic density decreases

downstream. Conversely, the vehicle undergoes a deceleration if the driver observes an increase in the traffic density along the road. The term $a(k,u)$ denotes the sensitivity of the traffic acceleration/deceleration to the gradient of the traffic density. Various traffic models, proposed in the past, can be classified with respect to the definition of $a(k,u)$. In the Greenshields' model, $a(k,u) = m^2 k$, where, m is a constant. In the Greenberg's model, the definition of a is: $a(k,u) = c^2/k$, where, c is a constant. Equations (1) and (2) are solved along with a set of boundary conditions on the traffic density and speed at the inlet of the road and initial conditions. The boundary condition is of the form: $k(x_0,t) = k_0(t)$ and $u(x_0,t) = u_0(t)$, where $k_0(t)$ and $u_0(t)$ are the traffic density and speed, respectively at the inlet of the road $(x = x_0)$. Similarly, the initial conditions are of the form: $k(x,t=0) = k^0(x)$ and $u(x,t=0) = u^0(x)$.

2.2 1-equation model: LWR model

In these models, one assumes that there exists an equilibrium speed-density relationship (i.e. $u = u(k)$). Therefore, $\frac{\partial q}{\partial x}$ may be expressed as $u_w \frac{\partial k}{\partial x}$, where, $u_w = \frac{dq}{dk}$. Equation (1) may be rewritten in the following form:

$$\frac{\partial k}{\partial t} + u_w \frac{\partial k}{\partial x} = 0 \tag{3}$$

Once the relationship, $u = u(k)$, is known the above equation may be utilized to track the spatio-temporal evolution of traffic density, k. A similar equation, for u, may be realized by assuming the relationship $k = k(u)$. Equation (3) can be cast in the following form:

$$\frac{\partial u}{\partial t} + u_w \frac{\partial u}{\partial x} = 0 \tag{4}$$

The $1-equation$ models are popularly known as LWR models [Lighthill and Whitham (1955) and Richards (1956)]. In this article we discuss two traffic models that are cast in this form: the Greenshields' (LWR_{GS}) and Greenberg's (LWR_{GB}) models. In the Greenshields' model, the speed-density relationship is given by $u_{GS}(k) = u_f(1 - \frac{k}{k_j})$. The $u - k$ relationship for the Greenberg model is: $u_{GB}(k) = c\ln(\frac{k_j}{k})$. Here, u_f is the free-flow speed (i.e. the hypothetical traffic speed for $k = 0$), c the speed at the maximum flux of traffic, and k_j the jam-density (i.e. traffic density for $u = 0$). The LWR models can either be expressed in terms of k, via Equation (3) or in terms of u, via Equation (4). This is identified by the superscript, k or u. Four LWR models are studied in this work: LWR_{GS}^u, LWR_{GS}^k, LWR_{GB}^u and LWR_{GB}^k. The boundary condition for LWR^k models is the specification of the incoming traffic density at the inlet of the road under consideration: $k(x_0,t) = k_0(t)$. Similarly, the

boundary condition for LWR^u models is $u(x_0,t) = u_0(t)$. Here, $k_0(t)$ and $u_0(t)$ are, respectively, the traffic density, and speed at the inlet of the road, $x = x_0$. The initial condition for LWR^k models is the specification of density over the entire road under consideration at the time instant, $t = 0$: $k(x,t = 0) = k^0(x)$. Similarly, the initial condition for LWR^u model is $u(x,t = 0) = u^0(x)$. Here, $k^0(x)$ and $u^0(x)$ are the variation of traffic density and traffic speed, respectively, over the entire domain at $t = 0$.

3   Finite element formulation

3.1   *2-equation models*

The domain, Ω, is discretized into subdomains Ω^e, $e = 1, 2, \ldots, n_{el}$, where n_{el} is the number of elements. A stabilized finite element method using piecewise linear interpolation functions is employed to discretize the governing equations. Let $\mathscr{V}_k^h$ and $\mathscr{V}_u^h$ represent the finite-dimensional variation space and $\mathscr{S}_k^h$ and $\mathscr{S}_u^h$ the solution space. These are defined as follows:

$$\mathscr{V}_k^h = \{w_k^h(x) \,|\, w_k^h \in H^{1h}(x),\, w_k^h(x_0) = 0\}, \tag{5}$$

$$\mathscr{V}_u^h = \{w_u^h(x) \,|\, w_u^h \in H^{1h}(x),\, w_u^h(x_0) = 0\}, \tag{6}$$

$$\mathscr{S}_k^h = \{k^h(x,t) \,|\, k^h(x,t) \in H^{1h}(x),\, k^h(x_0,t) = k_0(t)\}, \tag{7}$$

$$\mathscr{S}_u^h = \{u^h(x,t) \,|\, u^h(x,t) \in H^{1h}(x),\, u^h(x_0,t) = u_0(t)\}. \tag{8}$$

Here, $H^{1h}(\Omega) = \{\phi^h | \phi^h \in C^0(\Omega), \phi^h|_{\Omega^e} \in P^1, e = 1,2,\ldots,n_{el}\}$ and P^1 represents first-order polynomials. The stabilized finite element formulation of Equations (1) and (2) is as follows:

Find $k^h(x,t) \in \mathscr{S}_k^h$ and $u^h(x,t) \in \mathscr{S}_u^h$ such that $\forall w_k^h \in \mathscr{V}_k^h$ and $\forall w_u^h \in \mathscr{V}_u^h$

$$\int_\Omega w_k^h \left(\frac{\partial k^h}{\partial t} + u^h \frac{\partial k^h}{\partial x} + k^h \frac{\partial u^h}{\partial x} \right) d\Omega$$

$$+ \int_\Omega w_u^h \left(\frac{\partial u^h}{\partial t} + u^h \frac{\partial u^h}{\partial x} + a(k^h,u^h) \frac{\partial k^h}{\partial x} \right) d\Omega$$

$$+ \sum_{e=1}^{n_{el}} \int_{\Omega^e} \left(\tau_{kk} u^h \frac{\partial w_k^h}{\partial x} + \tau_{ku} \frac{\partial w_u^h}{\partial x} \right) \left(\frac{\partial k^h}{\partial t} + u^h \frac{\partial k^h}{\partial x} + k^h \frac{\partial u^h}{\partial x} \right) d\Omega^e$$

$$+ \sum_{e=1}^{n_{el}} \int_{\Omega^e} \left(\tau_{uu} u^h \frac{\partial w_u^h}{\partial x} + \tau_{uk} \frac{\partial w_k^h}{\partial x} \right) \left(\frac{\partial u^h}{\partial t} + u^h \frac{\partial u^h}{\partial x} + a(k^h,u^h) \frac{\partial k^h}{\partial x} \right) d\Omega^e$$

$$+ \sum_{e=1}^{n_{el}} \int_{\Omega^e} \left(\delta_{Sk} \frac{\partial k^h}{\partial x} \frac{\partial w_k^h}{\partial x} + \delta_{Su} \frac{\partial u^h}{\partial x} \frac{\partial w_u^h}{\partial x} \right) d\Omega^e = 0. \tag{9}$$

The first two terms of Equation (9) represent the Galerkin formulation of the governing equations. The remaining terms, that involve the element level integrals, are the stabilization terms that are added to the formulation to enhance the numerical stability of the basic Galerkin formulation. The terms with coefficients τ_{kk} and τ_{uu} are based on the well known SUPG (Streamline-Upwind/Petrov-Galerkin) stabilization [Brooks and Hughes (1982)]. They stabilize the computations in convection dominated flows. The terms with coefficients τ_{ku} and τ_{uk} are the IEPG (Inter-Equation/Petrov-Galerkin) stabilizations. These terms suppress the instabilities that arise out of coupling between the continuity and behavioral equations. It is shown later in the article that without these terms the computations may lead to node-to-node oscillations. To the best of the knowledge of the authors, it is for the first time that such a stabilization is being introduced. The terms with coefficients δ_{Sk} and δ_{Su} are the shock-capturing terms. The development of these terms are inspired by earlier articles [Juanes and Patzek (2005), Beau and Tezduyar (1991), Mittal (1998a), and Mittal (1998b)]. These term, by design, are active in the region of high gradients. The Galerkin formulation is known to lead to under- and over-shoots in the presence of shocks and large gradients. The shock capturing terms stabilize the computations in the presence of shocks/large gradients. The coefficients τ_{kk}, τ_{uu}, τ_{ku}, τ_{uk}, δ_{Sk}, and δ_{Su} are defined as follows:

$$\tau_{kk} = \tau_{uu} = \frac{h^e}{2|u^h|}, \tag{10}$$

$$\tau_{ku} = \frac{h^e}{2|u^h|}\, a(k^h, u^h), \tag{11}$$

$$\tau_{uk} = \frac{h^e}{2|u^h|}\, k^h, \tag{12}$$

$$\delta_{Sk} = \frac{h^e}{2}\, \frac{|\partial_t k^h + u^h\, \partial_x k^h + k^h\, \partial_x u^h|}{|\partial_x k^h|}, \tag{13}$$

$$\delta_{Su} = \frac{h^e}{2}\, \frac{|\partial_t u^h + u^h\, \partial_x u^h + a(k^h, u^h)\, \partial_x k^h|}{|\partial_x u^h|}, \tag{14}$$

Here, h^e is the element length. It is to be noted that the stabilized formulation is based on the residual of the governing equations. Therefore, it is consistent in the

sense that the exact solution is admitted by the formulation. This is also true for the shock capturing term; the coefficients, δ_{Sk} and δ_{Su}, are also based on the residual of the corresponding equations. The numerical integration of the various terms in the formulation is carried out via the Gauss-Legendre quadrature rule. The time integration of the equations is carried out via the Generalized Trapezoidal Rule. A second-order-in-time procedure is utilized for the computations.

3.2   1-equation (LWR) model

The $1 - equation$ model can be expressed in either k or u. Equation (3) represents the LWR^k model. The stabilized finite element formulation for the same is:
Find $k^h(x,t) \in \mathscr{S}_k^h$ such that $\forall w^h \in \mathscr{V}_k^h$

$$\int_\Omega w^h \left(\frac{\partial k^h}{\partial t} + u_w^h \frac{\partial k^h}{\partial x} \right) d\Omega + \sum_{e=1}^{n_{el}} \int_{\Omega^e} \tau u_w^h \frac{\partial w^h}{\partial x} \left(\frac{\partial k^h}{\partial t} + u_w^h \frac{\partial k^h}{\partial x} \right) d\Omega^e$$

$$+ \sum_{e=1}^{n_{el}} \int_{\Omega^e} \delta_k \frac{\partial w^h}{\partial x} \frac{\partial k^h}{\partial x} d\Omega^e = 0 \qquad (15)$$

Similarly, the stabilized finite element formulation for the LWR^u model, given by Equation (4) is:
Find $u^h(x,t) \in \mathscr{S}_u^h$ such that $\forall w^h \in \mathscr{V}_u^h$

$$\int_\Omega w^h \left(\frac{\partial u^h}{\partial t} + u_w^h \frac{\partial u^h}{\partial x} \right) d\Omega + \sum_{e=1}^{n_{el}} \int_{\Omega^e} \tau u_w^h \frac{\partial w^h}{\partial x} \left(\frac{\partial u^h}{\partial t} + u_w^h \frac{\partial u^h}{\partial x} \right) d\Omega^e$$

$$+ \sum_{e=1}^{n_{el}} \int_{\Omega^e} \delta_u \frac{\partial w^h}{\partial x} \frac{\partial u^h}{\partial x} d\Omega^e = 0 \qquad (16)$$

The first term in Equations (15) and (16) represent the Galerkin formulation of the governing equations. The terms involving the element level integrals are added to the formulation to enhance its numerical stability. The terms with coefficient τ are conventional SUPG (streamline-upwind/Petrov-Galerkin) terms while the ones involving δ are the shock-capturing terms. The stabilization coefficients are defined as follows:

$$\tau = \frac{h^e}{2|u_w^h|}, \qquad (17)$$

$$\delta_k = \frac{h^e}{2} \frac{|\partial_t k^h + u_w^h \partial_x k^h|}{|\partial_x k^h|}, \qquad (18)$$

$$\delta_u = \frac{h^e}{2} \frac{|\partial_t u^h + u^h_w \partial_x u^h|}{|\partial_x u^h|}. \tag{19}$$

As is the case with the stabilized formulation for $2-equation$ model, the formulation for LWR model is also based on the residual of the governing equation. Therefore, including the shock capturing term, it is consistent in the sense that the exact solution is admitted by the formulation. Unlike the formulation for $2-equation$ model, the formulation for the LWR model does not need the IEPG stabilization.

4   Numerical experiments

The proposed stabilized finite element formulation is applied to two classes of traffic models: LWR and 2-equation models. The performance of the two sets of models is compared. The role of the stabilization terms is demonstrated via numerical examples. It is also shown that certain models, that have been proposed earlier, suffer from an inconsistency in the presence of shocks.

Two models are utilized for modeling the the driver behavior: the Greenshields'- and Greenberg's-model (1959). In this paper, they are identified by the subscripts GS and GB, respectively. Both these models can be cast either as the LWR (Lighthill-Whitham-Richards) model or as a two-equation model ($2EQ$). Further, the LWR model may be represented either in terms of the traffic density, k, or the traffic speed: u. Thus, the Greenshields' model may be expressed in one of the three forms: LWR^k_{GS}, LWR^u_{GS} and $2EQ_{GS}$. The superscript in the LWR model represents the variable being used. For example, the LWR^k_{GS} model represents the Greenshields' model in the LWR form in terms of the variable k. It is expected that the Greenshields' model should produce very similar results in all the three forms. This is demonstrated in the first subsection below. The results from the Greenberg's model, however, throw a surprise. In the presence of a shock, the results from the LWR^k_{GB}, LWR^u_{GB} and $2EQ_{GB}$ exhibit differences in terms of the shock speed. This is investigated in a later subsection.

The models and their finite element implementations are tested on a road section of length 1000 m. The channel is discretized in 200 uniform linear elements; the element length is 5 m. The time step used is $\Delta t = 0.01$ s. The parameters free-stream speed (u_f), traffic jam density (k_j) and the constant c, in the behavioral model are 100 km/hr, 120 veh/km and 10 m/s, respectively. Two test cases are considered: (i) an expansion wave and (ii) shock wave. The initial and boundary conditions for the numerical experiments are listed in Table 1. The initial and boundary conditions are prescribed as per the corresponding traffic speed-density relationship for the two models: $u_{GS}(k) = u_f(1 - (k/k_j))$ and $u_{GB}(k) = c \ln(k_j/k)$.

Table 1: Initial and boundary conditions for various models in expansion wave and shock wave cases

	Expansion case			Shock case		
	Initial condition		Boundary	Initial condition		Boundary
Model	$x < 500$ m	$x \geq 500$ m	condition	$x < 500$ m	$x \geq 500$ m	condition
LWR_{GS}^k	$k = 90$	$k = 70$	$k = 90$	$k = 10$	$k = 70$	$k = 10$
LWR_{GS}^u	$u = u_{GS}(90)$	$u = u_{GS}(70)$	$u = u_{GS}(90)$	$u = u_{GS}(10)$	$u = u_{GS}(70)$	$u = u_{GS}(10)$
$2EQ_{GS}$	$k = 90,$ $u = u_{GS}(90)$	$k = 70,$ $u = u_{GS}(70)$	$k = 90,$ $u = u_{GS}(90)$	$k = 10,$ $u = u_{GS}(10)$	$k = 70,$ $u = u_{GS}(70)$	$k = 10,$ $u = u_{GS}(10)$
LWR_{GB}^k	$k = 90$	$k = 70$	$k = 90$	$k = 10$	$k = 70$	$k = 10$
LWR_{GB}^u	$u = u_{GB}(90)$	$u = u_{GB}(70)$	$u = u_{GB}(90)$	$u = u_{GB}(10)$	$u = u_{GB}(70)$	$u = u_{GB}(10)$
$2EQ_{GB}$	$k = 90,$ $u = u_{GB}(90)$	$k = 70,$ $u = u_{GB}(70)$	$k = 90,$ $u = u_{GB}(90)$	$k = 10,$ $u = u_{GB}(10)$	$k = 70,$ $u = u_{GB}(70)$	$k = 10,$ $u = u_{GB}(10)$

4.1 Greenshields' model: LWR and 2-equation models

4.1.1 Test case I: expansion wave

The initial and boundary conditions for the three models, LWR_{GS}^k, LWR_{GS}^u, and $2EQ_{GS}$, are listed in Table 1. The initial condition corresponds to a sudden drop in traffic density and rise in traffic speed, midway at the road. The change in the traffic density, at $t = 0$, takes place in one element; the density drops from 90 veh/km at $x = 495$ m to 70 veh/km at $x = 500$ m. The corresponding increase in traffic speed is from 25.0 km/hr to 41.7 km/hr. Figures 1 and 2 show the spatial variation of the traffic density and speed at various time instants. The results from all the three models are in good agreement.

In order to further evaluate the results, the streamwise location of the center of the expansion wave is tracked at various time instants. The traffic density varies between 70 veh/km and 90 veh/km. The x location of the point associated with the mean traffic density ($k = 80$ veh/km) is studied. The results from the three models are listed in Table 2 for three instants of time. The exact location of this traffic condition can be worked out from the Greenshields' model and is given as $[497.5 + (2u(k = 80) - u_f)t]$. The $x-$ locations for $t = 0$, $5s$ and $10s$, from this expression, are $x = 497.5m$, $451.2m$ and $404.91m$, respectively and are also listed in Table 2. It is seen that results from all the three models are in good agreement with the exact result. The *LWR* model based on traffic-speed, LWR_{GS}^u, seems to perform the best.
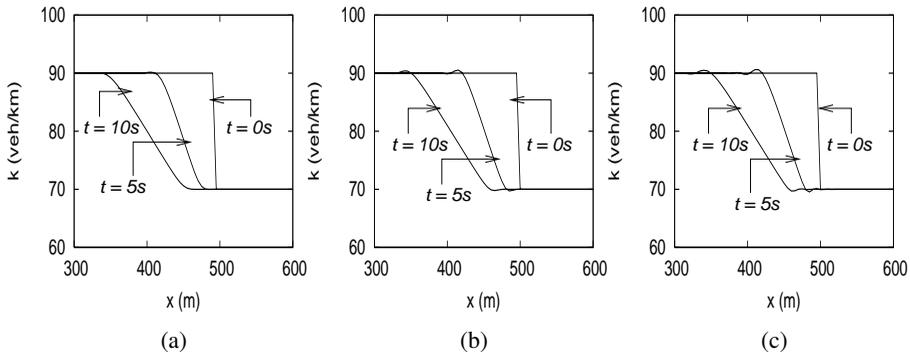
Figure 1: Evolution of expansion wave from the Greenshields' model: distribution of traffic density at various instants of time for the (a) LWR_{GS}^k, (b) LWR_{GS}^u, and (c) $2EQ_{GS}$ models.

Figure 2: Evolution of expansion wave from the Greenshields' model: distribution of traffic speed at various instants of time for the (a) LWR_{GS}^k, (b) LWR_{GS}^u, and (c) $2EQ_{GS}$ models.

Table 2: Location (in m) of the point with $k = 80$ veh/km (or $u = 33.3$ km/h) at two instants of time for various Greenshields' based traffic models.

Model	0 s	5 s	10 s
LWR_{GS}^k	497.50	451.43	405.16
LWR_{GS}^u	497.50	451.23	404.93
$2EQ_{GS}$	497.50	451.42	405.13
Exact	497.50	451.20	404.91
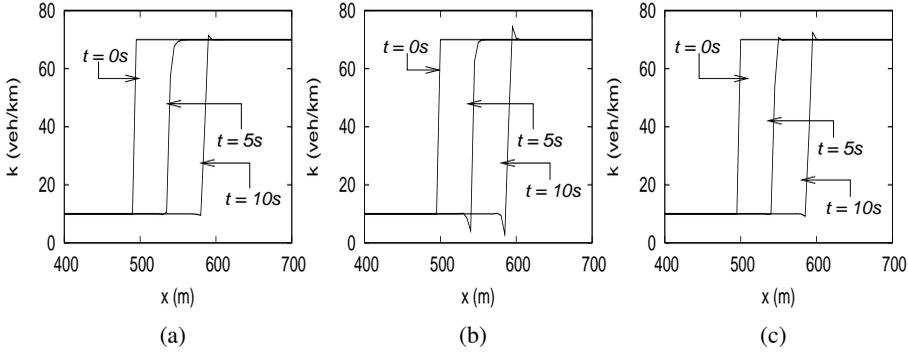
Figure 3: Propagation of shock wave from the Greenshields' model: distribution of traffic density at various instants of time for the (a) LWR^k_{GS}, (b) LWR^u_{GS}, and (c) $2EQ_{GS}$ models.

4.1.2   Test case II: shock wave

The initial and boundary conditions for the three models, LWR^k_{GS}, LWR^u_{GS}, and $2EQ_{GS}$, are listed in the second set of columns of Table 1. The initial condition corresponds to a sudden rise in traffic density and drop in traffic speed, midway at the road. The change in the traffic density, at $t = 0$, takes place in one element; the density rises from 10 veh/km at $x = 495$ m to 70 veh/km at $x = 500$ m. The corresponding decrease in traffic speed is from 91.7 km/hr to 41.7 km/hr. Figures 3 and 4 show the spatial variation of the traffic density and speed at various time instants. The downstream movement of the shock front is clearly observed. All the models lead to very comparable results. The over-shoots and under-shoots are smallest for the LWR^k_{GS} model and highest for the LWR^u_{GS} model.

To further evaluate the performance of the various models, the location of the shock wave is tracked at various time instants. For the same, the stream-wise location at which the traffic achieves a density of $k = 40$ veh/km is calculated. This corresponds to the mean of the two values of the traffic density at the two ends of the shock. The results for the three models, along with the exact location, are listed in Table 3 for three instants of time. It can be shown that the speed of the shock front is $u_{SW} = (q_1 - q_2)/(k_1 - k_2)$ where the subscripts 1 and 2 refer to the traffic conditions on either side of the shock. The streamwise location of the shock works out to $x_{SW} = 497.5 + u_{SW}t$. The $x-$location for $t = 0$, 5s and 10s, from this expression are $x = 497.5m$, $543.796m$ and $590.093m$, respectively and are also listed in Table 3. It is seen that the prediction of the location of the shock from all the three models is in good agreement with the exact result.
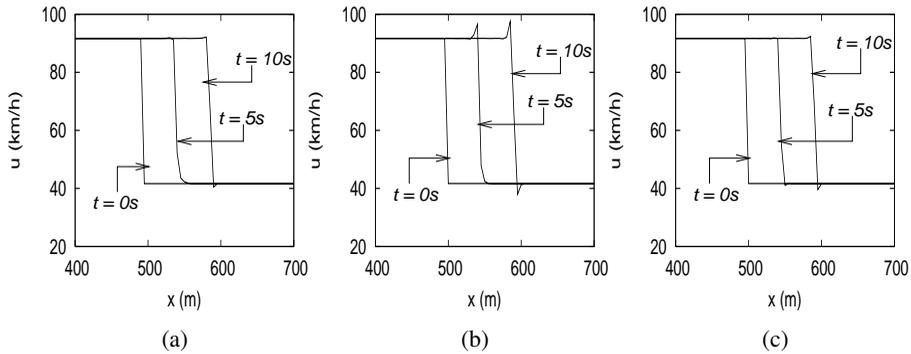
Figure 4: Propagation of shock wave from the Greenshields' model: distribution of traffic speed at various instants of time for the (a) LWR_{GS}^{k}, (b) LWR_{GS}^{u}, and (c) $2EQ_{GS}$ models.

Table 3: Location (in m) of shock front, based on the location of $k = 40$ veh/km or $u = 66.7$ km/h at two instants of time for various Greenshields' based traffic models.

Model	0 s	5 s	10 s
LWR_{GS}^{k}	497.50	543.14	590.26
LWR_{GS}^{u}	497.50	543.07	589.83
$2EQ_{GS}$	497.50	543.41	590.39
Exact	497.50	543.80	590.09
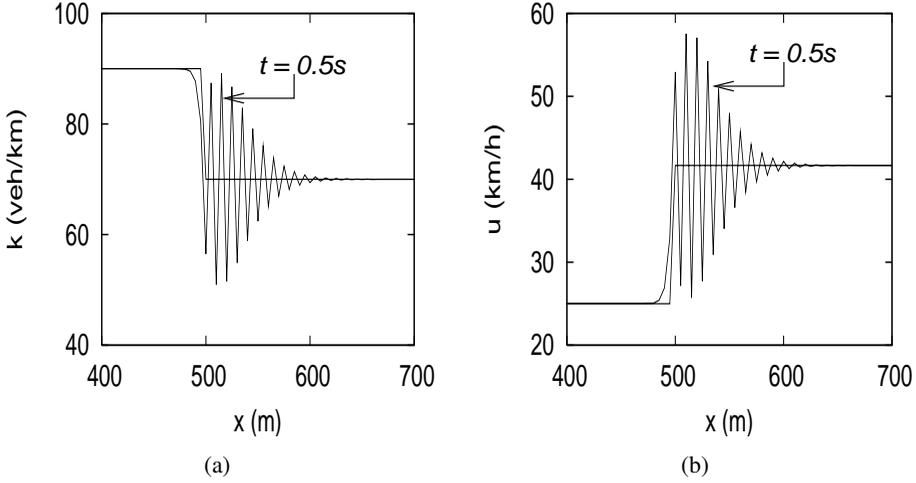
Figure 5: Evolution of node-to-node oscillation from FEM formulation by solving the $2EQ_{GS}$ model: distribution of traffic (a)density, and (b)speed at one instant of time; where FEM formulation excludes the cross-stabilization terms.

4.2 Role of the stabilization terms in the 2-equation model

Three kinds of stabilization terms are included in the formulation for the traffic model: SUPG (Streamline-Upwind/Petrov-Galerkin), shock capturing and IEPG (Inter-Equation/Petrov-Galerkin) stabilizations. While the first two are common to the formulations for the *LWR* and $2 - equation$ models, the inter-equation stabilization terms are unique to the $2 - equation$ model. The relevance of the shock capturing and *IEPG* stabilization terms is demonstrated in this subsection.

4.2.1 (IEPG) Inter-equation/Petrov-Galerkin stabilization

In Equation (9), the terms with coefficients τ_{ku} and τ_{uk} are the *IEPG* stabilizations. The expansion wave case, described in an earlier sub-section, is utilized to study the role of IEPG stabilization. Computations for this test case are carried out without the IEPG stabilization. The SUPG stabilization is, however, retained. Figure 5 shows the instantaneous fields for traffic speed and density at $t = 0$ and $0.5s$. Very large node-to-node oscillations can be observed in the solution. These oscillations grow with time. The solutions obtained with the IEPG stabilization included in the formulation are shown in Figures 1(c) and 2(c). These solutions are devoid of oscillations and clearly demonstrate the need of including the IEPG stabilization for the $2 - equation$ traffic model.
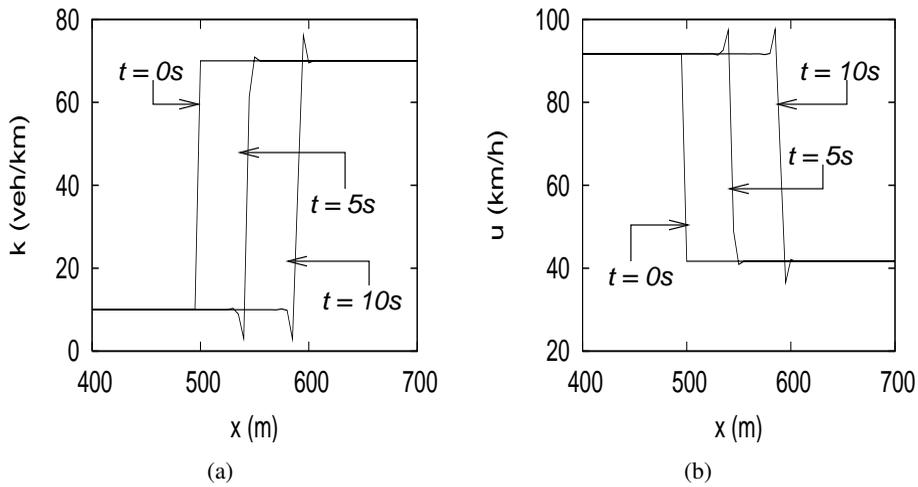
Figure 6: Propagation of shock wave having overshoots and undershoots from FEM formulation by solving $2EQ_{GS}$ model: distribution of traffic (a)density, and (b)speed at various instants of time; where FEM formulation excludes shock capturing terms.

4.2.2 *Shock-capturing term*

It is well known that the SUPG stabilizations are not adequate to prevent numerical oscillations when the solution is associated with shocks/discontinuities. Large over- and under-shoot may occur on the two sides of the shocks. Shock-capturing terms are included in the finite element formulation to handle such a situation. The test case-II related to the evolution of a shock wave in the traffic, described in an earlier sub-section, is utilized to study the role of shock-capturing stabilization in the context of the $2EQ_{GS}$. The terms with the coefficients δ_{Sk} and δ_{Su}, in Equation (9), are the shock-capturing terms. The shock-capturing coefficients, δ_{Sk} and δ_{Su}, are consistent in the sense that they are based on the residuals of the governing equations and vanish when an exact solution is achieved. Figure 6 shows the solution field for the traffic density and speed, at various time instants, without the shock-capturing terms. When this solution is compared to that presented in Figures 3(c) and 4(c), which are computed with the shock-capturing terms, a significant difference in the level of under- and over-shoots is observed. The computations with the shock-capturing terms included in the formulation (Figures 3(c) and 4(c)) have significantly lower oscillations on either side of the shock. This demonstrates the effectiveness of the shock-capturing stabilization. Similar observations are made for the LWR model as well.
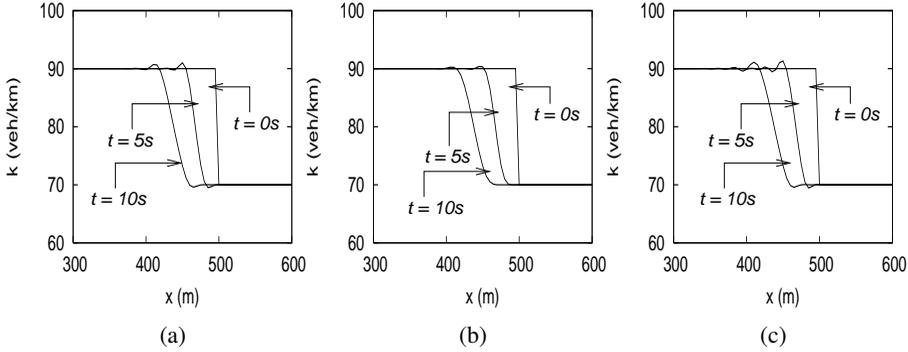
Figure 7: Evolution of expansion wave from the Greenberg model: distribution of traffic density at various instants of time for the (a) LWR_{GB}^k, (b) LWR_{GB}^u, and (c) $2EQ_{GB}$ models.

4.3 Greenberg model: LWR and 2-equation models

The stabilized finite element formulation is applied to the traffic flow where the driver behavior is assumed to follow the Greenberg model. Both, the *LWR* and $2 - equation$ models are studied. The test cases are the same as those studied for the Greenshields' model: expansion- and shock-wave. The details of the initial- and boundary conditions are listed in Table 1.

4.3.1 Test case I: expansion wave

At $t = 0$ the density drops from 90 veh/km at $x = 495$ m to 70 veh/km at $x = 500$ m. The corresponding increase in traffic speed is from 10.4 km/hr to 19.4 km/hr. Figures 7 and 8 show the spatial variation of the traffic density and speed at various time instants. The results from all the three models are in good agreement. The x location of the point associated with the mean traffic density ($k = 80$ veh/km) is studied. The results from the three models are listed in Table 4 for three instants of time. The exact location of this traffic condition can be worked out from the Greenberg's model. It is given by the expression: $[497.5 + (u(k = 80) - c)t]$ and the values at various time instants are listed in Table 4. The results from all the three models are in good agreement with the exact result. The *LWR* model based on traffic-density, LWR_{GB}^k, seems to perform the best.

4.3.2 Test case II: shock wave

The initial condition corresponds to a sudden rise in traffic density and drop in traffic speed, midway at the road. The traffic density, at $t = 0$, rises from 10 veh/km
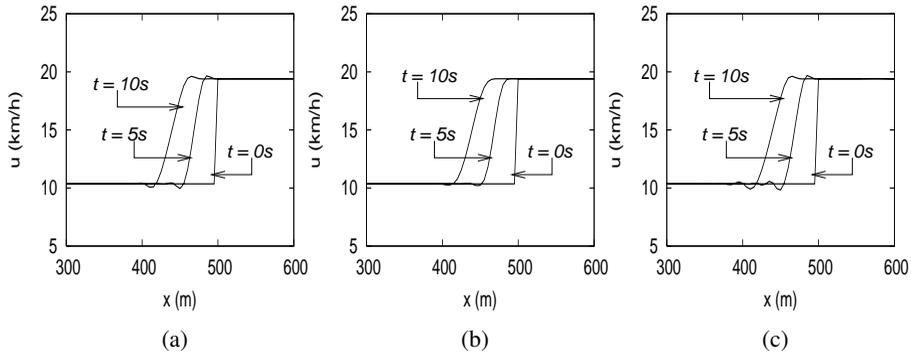
Figure 8: Evolution of expansion wave from the Greenberg model: distribution of traffic speed at various instants of time for the (a) LWR_{GB}^{k}, (b) LWR_{GB}^{u}, and (c) $2EQ_{GB}$ models.

Table 4: Location (in m) of the point with $k = 80 \; veh/km$ (or $u = 14.6 \; km/h$) at two instants of time for various Greenberg based traffic models.

Model	0 s	5 s	10 s
LWR_{GB}^{k}	497.50	467.65	437.97
LWR_{GB}^{u}	497.50	467.34	437.73
$2EQ_{GB}$	497.50	467.53	437.89
Exact	497.50	467.77	438.05
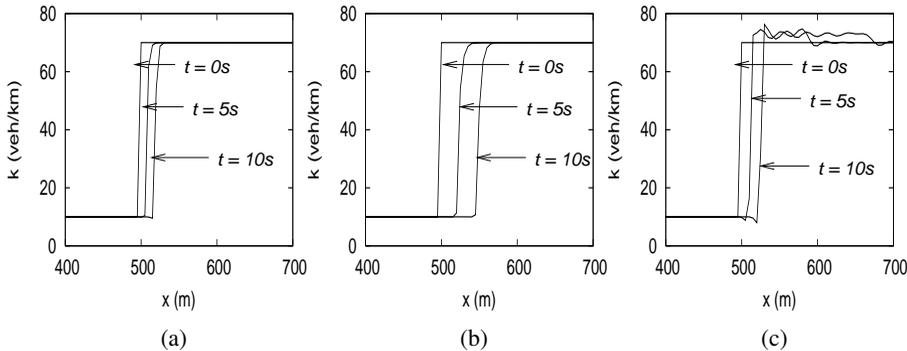
Figure 9: Propagation of shock wave from the Greenberg model: distribution of traffic density at various instants of time for the (a) LWR_{GB}^{k}, (b) LWR_{GB}^{u}, and (c) $2EQ_{GB}$ models.

at $x = 495\,m$ to $70\,veh/km$ at $x = 500\,m$. The corresponding decrease in traffic speed is from $89.5\,km/hr$ to $19.4\,km/hr$. Figures 9 and 10 show the spatial variation of the traffic density and speed at various time instants. It is observed from these figures that the LWR_{GB}^{k} and LWR_{GB}^{u} lead to different shock speeds. In fact, it can also be shown analytically that the shock speed for the traffic-density and traffic-speed are different for the Greenberg's model. In that sense the Greenberg's model is inconsistent in the presence of shocks. The undershoots and overshoots on the two sides of the shocks, therefore, also travel with different speeds for the two variables. This leads to the peculiar oscillations downstream of the shock for the $2EQ_{GB}$ model as observed in Figures 9(c) and 10(c).

The x location of the point associated with the mean traffic density ($k = 70\,veh/km$) and mean traffic speed ($u = 39.55\,km/h$) is studied to track the location of the shock. The results from the three models are listed in Table 5 for three instants of time. The exact location of this traffic condition can be worked out from the Greenberg's model. The shock speed for the u and k variables is different. The shock location for the two variables with the exact shock speed are also listed in the table. It is observed that the numerical solution from the LWR_{GB}^{k} is in good agreement with the exact solution for the k-variable. Similarly, the location of shock predicted by the LWR_{GB}^{u} model is in agreement with the exact solution for the u-variable. The shock from the $2EQ_{GB}$ model appears to travel at roughly the average of the shock speeds from the LWR_{GB}^{k} and LWR_{GB}^{u} models.
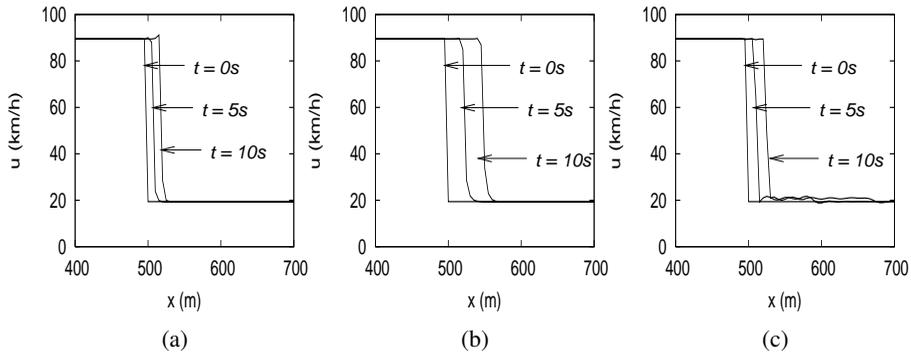
Figure 10: Propagation of shock wave from the Greenberg model: distribution of traffic speed at various instants of time for the (a) LWR^k_{GB}, (b) LWR^u_{GB}, and (c) $2EQ_{GB}$ models.

Table 5: Location (in m) of shock front, based on the location of $k = 40$ veh/km or $u = 39.55$ km/h at two instants of time for various Greenberg based traffic models.

Model	0 s	5 s	10 s
LWR^k_{GB}	497.50	507.87	518.41
$Exact(k)$	497.50	508.23	518.97
LWR^u_{GB}	497.50	524.03	549.45
$Exact(u)$	497.50	523.10	548.70
$2EQ_{GB}$	497.50	512.11	525.95
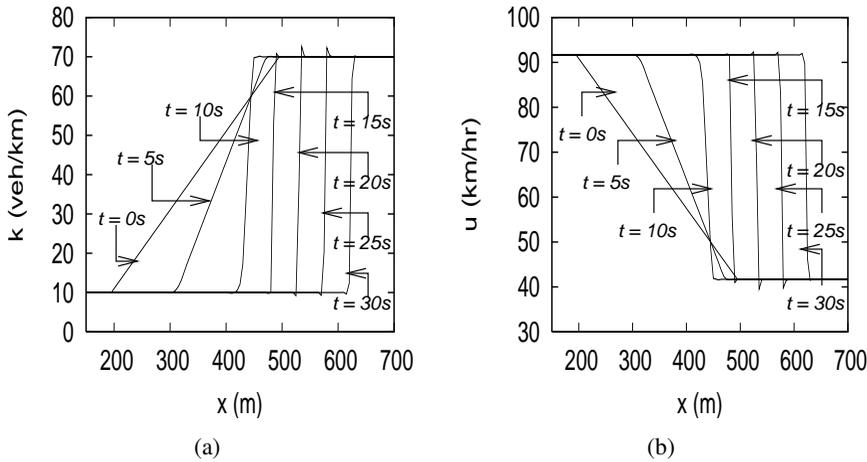
Figure 11: Evolution and then propagation of shock wave from the $2EQ_{GS}$ model: distribution of traffic (a)density, and (b)speed at various instants of time.

4.4 More on the inconsistency in the $2EQ_{GB}$ model

A test case is designed to bring out the inconsistency in the $2EQ_{GB}$ model. The computations begin with an initial condition corresponding to a linear increase, along a section of the road, in the traffic density. This condition evolves to a shock in the traffic speed and density. The performance of the $2EQ_{GB}$ model is studied during this evolution. The $2 - equation$ Greenshields' model, $2EQ_{GS}$, is put through a similar simulation to provide a case for comparison. The initial condition for the test case is as follows:

$$k(x,0) = \begin{cases} 10 \ veh/km & 0 \ m \leq x \leq 200 \ m \\ 10 + 0.2(x-200) \ veh/km & 200 \ m < x \leq 500 \ m \\ 70 \ veh/km & 500 \ m < x \leq 1000 \ m \end{cases}$$

The boundary condition is specified at the inlet of the road as $k(0,t) = 10 \ veh/km$. The corresponding conditions for u, for the initial- and boundary-condition, are computed from the $u-k$ relationship for the Greenberg and Greenshields' model, respectively.

Figure 11 show the spatial variation of the traffic density and speed at various time instants for the Greenshields' model. The linear ramp in the traffic density as well as speed, becomes steep with time and convects to a downstream location. Beyond $t \sim 10s$, the front evolves to a shock and travels to a further downstream location. The results for the simulation with the Greenberg model are shown in Figure 12.
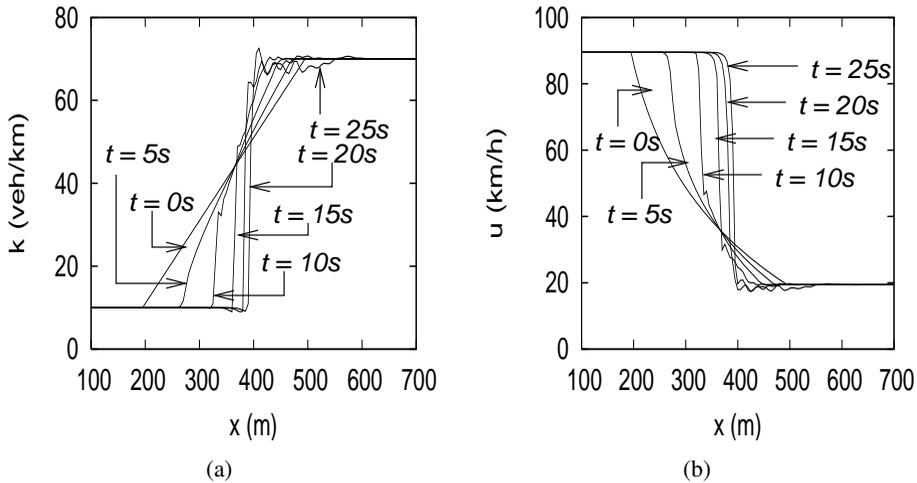
Figure 12: Evolution and then propagation of shock wave along with disturbances from the $2EQ_{GB}$ model: distribution of traffic (a)density, and (b)speed at various instants of time.

This figure shows the spatial variation of the traffic density and speed at various time instants. At $t = 0$, the spatial variation of density is linear. The traffic speed, at $t = 0$, is the one from the $u - k$ relationship for the Greenberg model and does not, therefore, vary linearly with distance. As is the case with the Greenshields' model, the spatial variation becomes steep with time and transitions towards a shock like front. So long the variation is gradual, the model works well. However, on the appearance of a shock, for $t \geq 10s$ oscillations develop in the solution. This is primarily because of the inconsistent shock speeds for the u and k variables in the Greenberg model, as highlighted earlier. This shows that the the Greenberg model behaves well as long as the variations in traffic condition are smooth. It, however, breaks down in the presence of shocks.

5   Concluding remarks

A stabilized finite element formulation has been presented to solve the governing equations for traffic flow. The flow of traffic is assumed to be one-dimensional. Both, PW-type (Payne-Whitham) 2-equation models and the LWR (Lighthill-Whitham-Richards) 1-equation models are considered. The LWR models can be either cast in terms of traffic density, k, or traffic speed, u. The finite element formulation for equations in either of the two variables is proposed. The Galerkin formulation is supplemented with SUPG (Streamline-Upwind/Petrov-Galerkin) and shock

capturing stabilizations. These are essential to suppress numerical instabilities associated with the Galerkin formulation in the advection dominated flows and in the presence of shocks. An additional stabilization for the 2-equation model is proposed. It arises out of coupling between the two equations and is termed as IEPG (Inter-Equation/Petrov-Galerkin) stabilization. All the stabilizations are based on the residual of the governing equations and are, therefore, consistent in the sense that the exact solution satisfies the finite element formulation. While the SUPG stabilization is well known, the IEPG stabilization has been proposed for the first time. The authors believe that this stabilization might be useful in other situations as well where there is a strong coupling between the various equations.

The stabilized formulation has been implemented and applied to various situations. Two models have been studied: Greenshields' (*GS*) and Greenberg's (*GB*) models. Numerical tests have been carried out for cases involving traffic expansion as well as shock with both models. Results have been computed with the $2EQ$, LWR^k and LWR^u formulations and compared. For the numerical test involving expansion of traffic, all the models work well and are in excellent agreement with the exact solution. The LWR^k_{GB} and LWR^k_{GS} give results that are closest to exact solution. It is shown that the $2EQ$ formulation without the $IEPG$ stabilization lead to large node-to-node oscillations. This demonstrates the need of the IEPG stabilization for the 2-equation traffic model. The need for including the shock capturing terms in all formulations is clearly demonstrated by the numerical test involving a traffic shock. The results from all the formulations are in very good agreement with the exact results for the Greenshields' model.

The computations with the Greenberg's (GB) model, in the presence of a shock, brings out an interesting point about the model that has not been reported earlier in the literature. It is found that the shock speed from the continuity and behavior equations, for the GB model, are different. In fact, the shock speeds from the LWR^u_{GB} and LWR^k_{GB} models for u and k, respectively are different. The values, for shock speed, obtained from the simulation with the LWR models very closely match the exact value for the two models for the respective variables. The shock, for the $2EQ_{GB}$ model, travels at roughly the average of the shock speeds from the LWR^u_{GB} and LWR^k_{GB} models. To further establish this inconsistency in the Greenberg's model, a test case is designed wherein the traffic flow evolves to a shock after a certain time. It is found that before the formation of shocks in the flow, till it is reasonably smooth, all formulations give the same solution. The inconsistency of the Greenberg's model becomes evident as soon as the shock appears in the flow.

References

Beau, G. J. L.; Tezduyar, T. E. (1991): Finite element computation of compressible flows with SUPG formulation. *Advances in Finite Element Analysis in Fluid Dynamics, ASME*, vol. 123, pp. 21–27.

Brackstone, M.; McDonald, M. (2000):   Car following: an historical review. *Transportation Research Part F*, vol. 2, no. 4, pp. 181–196.

Brooks, A. N.; Hughes, T. (1982):   Streamline upwind/Petrov-Galerkin formulations for convection dominated & flows with particular emphasis on the incompressible Navier-Stokes equations. *Comput. Meths. Appl. Mech. Engrg.*, vol. 32, pp. 199–259.

Daganzo, C. F. (1995):   A finite difference approximation of the kinematic wave model of traffic flow. *Transportation Research Part B*, vol. 29, pp. 261–276.

Greenberg, H. (1959):   An analysis of traffic flow. *Operations Research*, vol. 7, no. 1, pp. 79–85.

Jiang, R.; Wu, Q. S.; Zhu, Z. J. (2002):   A new continuum model for traffic flow and numerical tests. *Transportation Research Part B*, vol. 36, pp. 405–419.

Juanes, R.; Patzek, T. W. (2005):   Multiscale stabilized solutions to one-dimensional systems of conservation laws. *Comput. Meths. Appl. Mech. Engrg.*, vol. 194, pp. 2781–2805.

Leo, C. J.; Pretty, R. L. (1992):   Numerical simulations of macroscopic continuum traffic models. *Transportation Research Part B*, vol. 26, no. 3, pp. 207–220.

Lighthill, M. J.; Whitham, G. B. (1955):   On kinematic waves II. A theory of traffic flow on long crowded roads. *Proc. R. Soc.*, vol. 229, no. 1178, pp. 317–345.

Liu, C. S. (2006):   A group preserving scheme for Burgers equation with very large Reynolds number. *CMES: Computer Modeling in Engineering and Sciences*, vol. 12, no. 3, pp. 197–211.

Michalopoulos, P. G.; Beskos, D. E.; Lin, J. K. (1984):   Numerical simulations of macroscopic continuum traffic models. *Transportation Research Part B*, vol. 18, pp. 409–421.

Mittal, S. (1998):   Finite element computation of unsteady viscous compressible flows. *Comput. Methods Appl. Mech. Engrg.*, vol. 157, pp. 151–175.

Mittal, S. (1998):   Finite element computation of unsteady viscous compressible flows past & stationary airfoils. *Computational Mechanics*, vol. 21, pp. 172–188.

Papageorgiou, M. (1998):   Some remarks on macroscopic traffic flow modeling. *Transportation Research Part A*, vol. 32, no. 5, pp. 323–329.

Payne, H. J. (1971): Models of freeway traffic and control. *Mathematical models of Public Systems, Simulations Councils Proc. Ser.*, vol. 1, pp. 51–60.

Richards, P. I. (1956): Shock waves on the highway. *Operations Res.*, vol. 4, pp. 42–51.

Whitham, G. B. (1974): *Linear and Nonlinear waves*. Wiley, New York.

Zang, H. M. (1998): A theory of nonequilibrium traffic flow. *Transportation Research Part B*, vol. 32, pp. 485–498.

Zhang, H. M. (2001): A finite difference approximation of a non-equilibrium traffic flow model. *Transportation Research Part A*, vol. 35, pp. 337–365.

Zhang, P.; Wong, S. C. (2006): Essence of conservation forms in the traveling wave solutions of & higher-order traffic flow models. *Physical Review E*, vol. 74, no. 3, pp. 026109.